

Scalable Adversarial Attack Algorithms on Influence Maximization

Lichao Sun
lis221@lehigh.edu
Lehigh University
USA

Xiaobin Rui
ruixiaobin@cumt.edu.cn
China University of Mining and
Technology
China

Wei Chen
weic@microsoft.com
Microsoft Research
China

ABSTRACT

In this paper, we study the adversarial attacks on influence maximization under dynamic influence propagation models in social networks. In particular, given a known seed set S , the problem is to minimize the influence spread from S by deleting a limited number of nodes and edges. This problem reflects many application scenarios, such as blocking virus (e.g. COVID-19) propagation in social networks by quarantine and vaccination, blocking rumor spread by freezing fake accounts, or attacking competitor's influence by incentivizing some users to ignore the information from the competitor. In this paper, under the linear threshold model, we adapt the reverse influence sampling approach and provide efficient algorithms of sampling valid reverse reachable paths to solve the problem. We present three different design choices on reverse sampling, which all guarantee $1/2 - \epsilon$ approximation (for any small $\epsilon > 0$) and an efficient running time.

KEYWORDS

influence maximization, triggering model, greedy algorithm

1 INTRODUCTION

Influence maximization (IM) is the optimization problem of finding a small set of most influential nodes in a social network that generates the largest influence spread, which has many applications such as promoting products or brands through viral marketing in social networks [10, 16, 22]. However, in real life, there are so many competitions in various scenarios with different purposes, such as attacking competitor's influence [18], controlling rumor [4, 14] or blocking the virus spread. The adversary will block the virus propagation by quarantine and vaccination, block rumor spread by freezing fake accounts, or attack competitors' influence by incentivizing some users to ignore the information from the competitor. All these scenarios can be modeled as the adversary trying to remove certain nodes and edges to minimize the influence or impact from the competitor's seed set in social networks, which we denoted as the adversarial attacks on influence maximization (AdvIM).

We model the AdvIM task more formally as follows. The social influence network is modeled as a weighted network $G = (V, E, w)$, where V is a set of nodes representing individuals, E is a set of directed edges representing influence relationships, and w is influence weights on edges. At the beginning, we have a fixed seed set S , and the propagation from S follows the classical linear threshold model [16]. For an attack set A consisting of a mix of nodes (disjoint from S) and edges, we measure the effectiveness of A by the *influence reduction* $\rho_S(A)$ it achieves, which is defined as the difference in influence spread with and without removing nodes and edges in

the attack set A . Then, given a node budget q_N and an edge budget q_E , the AdvIM task is to find an attack set A with at most q_N nodes (excluding any seed node) and at most q_E edges, such that after removing the nodes and edges in A , the influence spread of S is minimized, or the *influence reduction* $\rho_S(A)$ is maximized.

We show that under the LT model, the influence reduction function $\rho_S(A)$ is monotone and submodular, which enables a greedy approximation algorithm. However, direct greedy algorithm is not efficient since it requires a large number of simulation of propagations from the seed set S . In this paper, we adapt the reverse influence sampling (RIS) approach to design efficient algorithms for the AdvIM task. Due to the nature of the problem, only successful propagation from the seed set can be potentially reduced by the attack set. This creates a new challenge for reverse sampling. In this paper, we present three different design choices for such reverse sampling and their theoretical analysis. They all provide a $1/2 - \epsilon$ approximation guarantee, and have different trade-offs in efficiency guarantee. We then conduct experimental evaluation on several real-world networks and demonstrate that our algorithms achieves good influence reduction results while running much faster than existing greedy based algorithms. To summarize, *our contributions* are: (a) proposing the study of adversarial attacks on influence maximization problems; (b) designing efficient algorithms by adapting the RIS approach and providing their theoretical guarantees; and (c) conducting experiments on real-world networks to demonstrate the effectiveness and the efficiency of our proposed algorithms.

Related Work. Domingos and Richardson first studied Influence Maximization (IM) [10, 22], and then IM is mathematically formulated as a discrete optimization problem by Kempe et al. [16], who also formulate the independent cascade model, the linear threshold model, the triggering model, and provide a greedy approximation algorithm based on submodularity. After that, most works focus on improving the efficiency and scalability of influence maximization algorithms [3, 8, 9, 15, 25, 26, 28]. The most recent and the state of the art is the reverse influence sampling (RIS) approach [3, 21, 24–26], and the IMM algorithm of [25] is one of the representative algorithms for the RIS approach. Some other studies look into different problems, such as competitive and complementary influence maximization [4, 6, 12, 14, 19, 27], adoption maximization [2], robust influence maximization [7, 13], etc. The most similar topic to this work is competitive influence maximization that aims to maximize the influence while more than one party is in the social network.

One similar work also wants to stop the influence spread in the social network [17]. However, this work has a different objective

function that estimates the total influence by summing up the influence of the individual node in seed sets, which is different from the traditional influence maximization. They proposed the greedy approach through forward-tree simulation without time-complexity analysis. In this work, our objective function directly matches the original influence maximization objective function. Moreover, we propose RIS-based algorithms to overcome the efficiency issue in the forward simulation approach while also providing theoretical guarantee on both the approximation ratio and the running time. Through experimental analysis, we find the forward simulation algorithms is not effective and efficient in general, comparing to our RIS-based algorithms.

2 MODEL AND PROBLEM DEFINITION

Adversarial Attacks on Diffusion Model. In this paper, we focus on the well-studied *linear threshold (LT) model* [16] as the basic diffusion model. A social network under the LT model is modeled as a directed influence graph $G = (V, E, w)$, where V is a finite set of vertices or nodes, $E \subseteq V \times V$ is the set of directed edges connecting pairs of nodes, and $w : E \rightarrow [0, 1]$ gives the influence weights on all edges. The diffusion of information or influence proceeds in discrete time steps $t = 0, 1, 2, \dots$. At time $t = 0$, the seed set S_0 is selected to be active, and also each node v independently select a threshold θ_v uniformly at random in the range $[0, 1]$, corresponding to users' true thresholds. At each time $t \geq 1$, an inactive node v becomes active if $\sum_{u:u \in S_{t-1}, (u,v) \in E} w(u, v) \geq \theta_v$ where S_{t-1} is the set of nodes activated by time $t - 1$. The diffusion process ends when there is no more nodes activated in a time step.

Given the weights of all nodes $v \in V$, we can construct the live-edge graph $L = (V, E(L))$, where at most one of each v 's incoming edges is selected with probability $w(u, v)$, and no edge is selected with probability $1 - \sum_{u:(u,v) \in E} w(u, v)$. Each edge $(u, v) \in L$ is called a *live edge*. Kempe et al. [16] show that the propagation in the linear threshold model is equivalent to the deterministic propagation via breadth-first traversal in a random live-edge graph L . An important metric in a diffusion model is the *influence spread*, defined as the expected number of active nodes when the propagation from the given seed set S_0 ends, and denoted as $\sigma(S_0)$. Let $\Gamma(G, S)$ denote the set of nodes in graph G that can be reached from the node set S . Then, by the above equivalent live-edge graph model, we have $\sigma(S_0) = \mathbb{E}_L[|\Gamma(L, S_0)|] = \sum_L \Pr[L|G] \cdot |\Gamma(L, S_0)|$, where the expectation is taken over the distribution of live-edge graphs, and $\Pr[L|G]$ is the probability of sampling a particular live-edge graph L in graph G . As what we defined above, we have:

$$p(v, L, G) = \begin{cases} w(u, v), & \text{if } \exists u : (u, v) \in L \\ 1 - \sum_{u:(u,v) \in E} w(u, v), & \text{otherwise} \end{cases}$$

which is the probability of the configuration of incoming edges for node v in L ; then, the probability of a particular live-edge graph L is $\Pr[L|G] = \prod_{v \in V} p(v, L, G)$. When we need to specify the graph, we use $\sigma(S_0, G)$ to represent the influence spread under graph G .

A set function $f : V \rightarrow \mathbb{R}$ is called *submodular* if for all $S \subseteq T \subseteq V$ and $u \in V \setminus T$, $f(S \cup \{u\}) - f(S) \geq f(T \cup \{u\}) - f(T)$. Intuitively, submodularity characterizes the diminishing return property often occurring in economics and operation research. Moreover, a set function f is called *monotone* if for all $S \subseteq T \subseteq V$, $f(S) \leq f(T)$. It is

shown in [16] that influence spread σ for the linear threshold model is a monotone submodular function. A non-negative monotone submodular function allows a greedy solution to its maximization problem subject to a cardinality constraint, with an approximation ratio $1 - 1/e$, where e is the base of the natural logarithm [20]. This is the technical foundation for most influence maximization tasks.

Adversarial Attacks on Influence Maximization. The classical influence maximization problem is to choose a seed set S of size at most k seeds to maximize the influence spread $\sigma(S, G)$. For the Adversarial Attacks Influence Maximization (AdvIM) problem, the goal is to select at most q_N nodes and q_E edges to be removed, such that the influence spread on a given seed set S is minimized. Let A denote a joint *attack set*, which contains a subset of nodes $A_N \subseteq V \setminus S$ and a subset of edges $A_E \subseteq E$, i.e. $A = A_N \cup A_E$. Denote the new graph after removing the nodes and edges in A as $G' = G \setminus A$. We first define the key concept of influence reduction under the attack set A .

Definition 1 (Influence Reduction). *Given a seed set S , the influence reduction under the attack set A , denoted as $\rho_S(A)$, is the reduction in influence spread from the original graph G to the new graph $G' = G \setminus A$. That is, $\rho_S(A) = \sigma(S, G) - \sigma(S, G \setminus A)$.*

Note that $S \cap A = \emptyset$, which means we cannot attack any seed node. We can now define the main optimization task in this paper.

Definition 2. *The Adversarial Attacks on Influence Maximization (AdvIM) under the linear threshold model is the optimization task where the input includes the directed influence graph $G = (V, E, w)$, seed set S , attack node budget q_N and attack edge budget q_E . The goal is to find an attack set A to remove, which contains at most q_N nodes (excluding the seed set S) and q_E edges, such that the total influence reduction is maximized: $A^* = \operatorname{argmax}_{A:|A_N| \leq q_N, |A_E| \leq q_E} \rho_S(A)$.*

Before the algorithm design, we first establish the important fact that influence reduction $\rho_S(A)$ as a set function is monotone and submodular.

Lemma 1. *Influence reduction $\rho_S(A)$ for the LT model satisfies monotonicity and submodularity.*

The monotonicity and submodularity above provides the theoretical basis for our efficient algorithm design, to be presented in the next section. All proofs and related materials are shown in the appendix.

3 EFFICIENT ALGORITHMS FOR ADVIM

The monotonicity and submodularity of the objective function enables the greedy approach for the maximization task. However, as commonly seen in influence maximization research, naively doing a greedy algorithm directly on the objective function is often very slow and not efficient, because the function evaluation requires a large number of Monte Carlo simulations to be accurate. In this section, we aim to speed up the greedy approach by adapting the approach of reverse influence sampling (RIS) [3, 25, 26], which provides both theoretical guarantee and efficiency. We first provide a general adversarial attack algorithm framework **AAIMM** based on IMM [25] in Section 3.1 (Algorithm 1). **AAIMM** relies on valid reverse reachable (VRR) path sampling. Then in Section 3.2, we provide several concrete implementations of VRR path sampling.

3.1 Algorithm Framework AAIMM

All efficient influence maximization algorithms such as IMM are based on the RIS approach, which generates a suitable number of reverse-reachable sets for influence estimation. In our case, we need to adapt the RIS approach for generating reverse-reachable paths in the LT model. Let S be the fixed seed set. Let L be a random live-edge graph generated from $G = (V, E, w)$ following the LT model. Recall that each node selects at most one incoming edge as a live edge in L . Thus, starting from a node $v \in V$, we may find at most one node u_1 such that $(u_1, v) \in L$. Let $u_0 = v$. In general, starting from $u_i \in V$, we may find at most one node $u_{i+1} \in V$ with $(u_{i+1}, u_i) \in L$. This process stops at some node u_j when one of the following conditions hold: (a) u_j is a seed node, i.e. $u_j \in S$; (b) there is no edge $(u, u_j) \in E(L)$; or (c) the path loops back, that is, the only edge $(u, u_j) \in E(L)$ satisfies $u \in \{u_0, \dots, u_{j-1}\}$. We call this process a reverse simulation from root v in the LT model, and the path obtained from u_j to u_0 a *reverse-reachable path (RR path) rooted at v* (under the live-edge graph L), denoted as $P_{L,v}$. Note that if L is a random live-edge graph, then $P_{L,v}$ is a random path, with randomness coming from L . When we do not specify the root v , we define a *reverse-reachable path (RR path)* (under a random live-edge graph L) P_L as a random $P_{L,v}$ with v selected uniformly at random from the node set $V \setminus S$. The reason we exclude the seed set S is because the root v selected in an RR path is to be used as a measure for the influence reduction of attack nodes or edges on the path, and since no seed node is selected in the attack set, no seed node will be counted for influence reduction. This point will be made clearly formally in the following lemma. Sometimes we omit the subscript L in P_L when the context is clear. Let $VE(P_L)$ be the joint set of nodes and edges of RR path P_L excluding any seed node.

We say that an RR path P_L is a valid RR path or VRR path which contains a seed node in S ; otherwise P_L is invalid. Intuitively, for a VRR path P_L , the influence of S can reach the root v of P_L through the path, and thus attacking any node or edge on the path would reduce the influence to v ; but if P_L is invalid, attaching a node or edge on P_L will not reduce the influence to v since anyway v is not influence by S . For convenience, sometimes we also use the notation of S -conditioned RR path P_L^S , which is P_L when P_L is valid and \emptyset when P_L is invalid. Let \mathcal{P}^S be the probability subspace of VRR paths. Let $n^- = |V| - |S|$, $\mathbb{I}\{\cdot\}$ be the indicator function, and $\sigma^-(S) = \sigma(S) - |S|$. The following lemma connects the influence reduction of an attack set A with the VRR paths.

Lemma 2. *For any given seed set S and attack set A ,*

$$\begin{aligned} \rho_S(A) &= n^- \cdot \mathbb{E}_L [\mathbb{I}\{A \cap VE(P_L^S) \neq \emptyset\}] \\ &= \sigma^-(S) \cdot \mathbb{E}_L [\mathbb{I}\{A \cap VE(P_L) \neq \emptyset\} \mid S \cap VE(P_L) \neq \emptyset]. \end{aligned}$$

The above property implies that we can sample enough RR path from the original space or VRR path from subspace \mathcal{P}^S to accurately estimate the influence reduction of A . More importantly, by Lemma 2 the optimal attack set can be found by seeking the optimal set of nodes and edges that intersect with (a.k.a. cover) the most number of VRR paths, which is a max-cover problem. Therefore, following the RIS approach, we turn the influence reduction maximization problem into a max-cover problem. We use the IMM algorithm [25] as the template, but other RIS algorithms follow the similar structure. Our algorithm AAIMM contains two phases,

Algorithm 1: AAIMM: Adversarial Attacks IMM

```

Input: Graph  $G = (V, E, w)$ , seed set  $S$ , budgets  $q_N, q_E$ ,  

accuracy parameters  $(\varepsilon, \ell)$ 
// Phase 1: Estimate  $\theta$ , the number of VRR paths needed, and
generate these VRR paths
1  $\mathcal{R} \leftarrow \emptyset$ ;  $LB \leftarrow 1$ ;  $\varepsilon' \leftarrow \sqrt{2}\varepsilon$ ; using binary search to find a  $\gamma$   

such that  $\lceil \lambda^*(\ell) \rceil / n^{\ell+\gamma} \leq 1/n^\ell$   $\ell \leftarrow \ell + \gamma + \ln 2/\ln n^-$ ;
2 for  $i = 1$  to  $\log_2(n-1)$  do
3    $x_i \leftarrow n^-/2^i$ ;
4    $\theta_i \leftarrow \lambda'/x_i$ ; //  $\lambda'$  is defined in Eq. (1)
5   while  $|\mathcal{R}| < \theta_i$  do
6     Sample a VRR path  $P$  from subspace  $\mathcal{P}^S$ , and insert
     it into  $\mathcal{R}$ ;
7    $A_i \leftarrow \text{NodeEdgeSelection}(\mathcal{R}, q_N, q_E)$ ;
8   if  $n^- \cdot F_{\mathcal{R}}^S(A_i) \geq (1 + \varepsilon') \cdot x_i$  then
9      $LB \leftarrow n^- \cdot F_{\mathcal{R}}^S(A_i)/(1 + \varepsilon')$ ;
10    break;
11  $\theta \leftarrow \lambda^*(\ell)/LB$ ; //  $\lambda^*(\ell)$  is defined in Eq. (2)
12 while  $|\mathcal{R}| \leq \theta$  do
13   Sample a VRR path  $P$  from subspace  $\mathcal{P}^S$ , and insert it
   into  $\mathcal{R}$ ;
// Phase 2: select attack nodes and edges from the generated
VRR paths
14  $A \leftarrow \text{NodeEdgeSelection}(\mathcal{R}, q_N, q_E)$ ;
15 return an attack set  $A$ 

```

estimating the number of VRR paths needed and greedy selection via max-cover, as shown in Algorithm 1. The two main parameters λ' and $\lambda^*(\ell)$ used in the algorithm are given below:

$$\lambda' \leftarrow \left[(2 + \frac{2}{3}\varepsilon') \cdot \left(\ln \left(\binom{n^-}{q_N} \binom{m}{q_E} \right) + \ell \cdot \ln n^- + \ln \log_2 n^- \right) \cdot n^- \right] / \varepsilon'^2 \quad (1)$$

$$\lambda^*(\ell) \leftarrow 2n \cdot (1/2 \cdot \alpha + \beta)^2 \cdot \varepsilon^{-2} \quad (2)$$

$$\alpha \leftarrow \sqrt{\ell \ln n + \ln 2}; \beta \leftarrow \sqrt{1/2 \cdot \left(\ln \left(\binom{n^-}{q_N} \binom{m}{q_E} \right) + \alpha^2 \right)}.$$

In Phase 1, we generate θ valid VRR paths \mathcal{R} , where θ is computed to guarantee the approximation with high probability. In Phase 2, we use the greedy algorithm to find the q_N nodes and q_E edges that cover the most number of VRR paths. This greedy algorithm is similar to prior algorithms, and thus we omit it here. Phase 1 follows the IMM structure to estimate a lower bound of the optimal value, which is used to determine the number of VRR paths needed. The main difference is that we need to sample valid RR paths, not the simple RR sets as before. This part will be discussed separately in the next section. Moreover, our solution space now is $\binom{n^-}{q_N} \binom{m}{q_E}$, and thus we replace the $\binom{n}{k}$ in the original IMM algorithm. Let A^* be the optimal solution of the AdvIM problem, and $\text{OPT} = \rho_S(A^*)$.

Lemma 3. For every $\varepsilon > 0$ and $\ell > 0$, to guarantee the approximation ratio with probability at least $1 - \frac{1}{n^\ell}$, the number of VRR paths needed by AAIMM is $O\left(\frac{(q_N \log n^- + q_E \log m + \ell \log n^-) \cdot \sigma^-(S)}{\text{OPT} \cdot \varepsilon^2}\right)$.

The special cases of adversarial attacks on influence maximization is attacking nodes only or edge only, i.e. $q_N = 0$ or $q_E = 0$. Then, the greedy algorithms of the special cases can achieve at least $(1 - 1/e - \varepsilon)$ of the optimal performance. However, our greedy algorithms for the AdvIM attacks both nodes and edges together. The idea of our greedy approach is that at every greedy step, it searches all nodes and edges (excluding the seed nodes) in the candidate space C and picks the one having the maximum marginal influence deduction. If the budget for node or edge exhausts, then the remaining nodes or edges are removed from C . Note that as C contains nodes and edges assigning to different partitions, AAIMM selects nodes or edges crossing partitions. This falls into a greedy algorithm subject to a partition matroid constraint, which is defined below.

Given a set U partitioned into disjoint sets U_1, \dots, U_n and $\mathcal{I} = \{X \subseteq U: |X \cap U_i| \leq k_i, \forall i \in [n]\}$, (U, \mathcal{I}) is called a *partition matroid*. Thus, the node and edge space \mathcal{A} with the constraint of AdvIM, namely $(\mathcal{A}, \{A: |A_N| \leq q_N, |A_E| \leq q_E\})$, is a partition matroid. This indicates that AdvIM is an instance of submodular maximization under partition matroid, which can be solved by a greedy algorithm with $1/2$ -approximation guarantee [11]. Using this result, we can obtain the result for our AAIMM algorithm.

Theorem 1. For every $\varepsilon > 0$ and $\ell > 0$, with probability at least $1 - \frac{1}{n^\ell}$, the output A^o of the AAIMM algorithm framework satisfies $\rho_S(A^o) \geq \left(\frac{1}{2} - \varepsilon\right) \rho_S(A^*)$. In this case, the expected running time for AAIMM is $O\left(\frac{(q_N \log n^- + q_E \log m + \ell \log n^-) \cdot \sigma^-(S)}{\text{OPT} \cdot \varepsilon^2} \cdot \text{ERPV}\right)$, where ERPV is the mean time of generating a VRR path.

Theorem 1 summarizes the theoretical guarantee of the approximation ratio and the running time of our algorithm framework AAIMM. Because we are attacking both nodes and edges with separate budgets, our approximation guarantee is $1/2 - \varepsilon$. If we only attack nodes (i.e. $q_E = 0$) or only attack edges (i.e. $q_N = 0$), then we could achieve the approximation ratio of $1 - 1/e - \varepsilon$. The running time result includes OPT. Although OPT cannot be obtained in general, it still provides the precise idea on the running time, and is useful to compare different implementations. In the next section, we will discuss concrete implementations of the VRR path sampling method, and in some cases we will fully realize the time complexity.

3.2 VRR Path Sampling

VRR path sampling is the key new component to fully realize our AAIMM algorithm. Here, we discuss three methods and their guarantees, and empirically evaluate these methods in our experiments.

Naive VRR Path Sampling. The first implementation is naively generate a RR path P starting from a random root $v \in V \setminus S$, and if P is valid then return it; otherwise regenerate a new path (see Algorithm 2). It is easy to see that to generate one VRR path, we need to generate a number of RR paths. Let ERP be the expected running time of generating one RR path. By a simple argument based on live-edge graphs, we can get that on average we need to

generate $n^-/\sigma^-(S)$ RR paths to obtain one VRR path that reaches the seed set S . This means $\text{ERPV} = \text{ERP} \cdot n^-/\sigma^-(S)$.

Theorem 2. *Naive VRR path sampling* (Algorithm 2) correctly samples a VRR path. The expected running time of AAIMM with naive VRR path sampling (Algorithm 2) is

$$O\left(\frac{(q_N \log n^- + q_E \log m + \ell \log n^-) \cdot n^-}{\text{OPT} \cdot \varepsilon^2} \cdot \text{ERP}\right). \quad (3)$$

Algorithm 2: Naive-VRR-Path: Naive VRR Path Sampling

Input: Graph G , seed set S
1 repeat
2 Randomly select a root $v \in V \setminus S$, and generate the reverse-reachable path P rooted at v ;
3 until $P \cap S \neq \emptyset$;
4 return a VRR path P .

Forward-Backward VRR Path Sampling. To avoid wasting RR path samplings as in the naive method, we can first do a forward simulation from S to generate a forward forest, recording the nodes and edges that a forward simulation from S will pass. Then, when randomly selecting a root v , we restrict the selection to be among the nodes touched by the forward simulation. Finally, the VRR path is the path from S to v recorded in the forward forest. This is the forward-backward sampling method given in Algorithm 3. Let $\text{EFF}(S)$ be the mean time of generating a forward forest from seed set S . Then we have the following result on this method.

Theorem 3. *Forward-backward VRR path sampling* (Algorithm 3) correctly samples a VRR path. The expected running time of AAIMM with forward-backward VRR path sampling (Algorithm 3) is

$$O\left(\frac{(q_N \log n^- + q_E \log m + \ell \log n^-) \cdot \sigma^-(S)}{\text{OPT} \cdot \varepsilon^2} \cdot \text{EFF}(S)\right). \quad (4)$$

Algorithm 3: FB-VRR-Path: Forward-Backward VRR Path Sampling

Input: Graph G , seed set S
1 Initialize an empty forest F ;
2 Forward propagating a new forest F by using LT model with S and G ;
3 Randomly select a node $v \in F \setminus S$, and set path P to be the one from S to v in the forest F ;
4 $\mathcal{R}^o \leftarrow \mathcal{R}^o \cup P$; return a VRR path P .

Comparing with naive sampling, the forward-backward sampling saves those sampling of invalid RR paths. However, it needs to generate a complete forward forest first, which is more expensive than generating one reverse path. Therefore, there is a tradeoff between the forward-backward method and the naive method, and the tradeoff is exactly quantified by their running time results: If $\text{EFF}(S)/\text{ERP} < n^-/\sigma^-(S)$, then the forward-backward method is faster; otherwise, the naive method is faster. Therefore, which one is better will depend on the actual graph instance.

Since the forward-backward method generates a forward forest first, one may be tempted to sample more VRR paths from this forest, but it will generate correlations among these VRR paths. Another attempt of generating a number of forward forests to record the frequencies of node appearances, and then use these frequencies to guide the RR path sampling would also deviate from the subspace probability distribution \mathcal{P}^S , and thus these methods would not provide theoretical guarantee of the overall correctness of **AAIMM**.

Reverse-Reachable Simulation with DAG. The naive method above wastes many invalid RR path samplings, while the forward-backward method wastes many branches in the forward forest. Thus, we desire a method that could do a simple VRR path sampling without such wastes. For directed-acyclic graphs (DAGs), we do discover such a VRR path sampling method by re-weighting edges.

Suppose G is a directed acyclic graph. As shown in [9], in a DAG, influence spread of a seed set can be computed in linear time. Let $ap_v(S)$ be the probability of v being activated when S is the seed set. Let $N^-(v)$ be the set of v 's in-neighbors. Then in a DAG G , we have $ap_v(S) = \sum_{u \in N^-(v)} ap_u(S) \cdot w(u, v)$. The above computation can be carried out with one traversal of the DAG in linear time from the seed set S following any topological sort order. For a DAG G , we propose the following sampling of a VRR path in \mathcal{P}^S as DAG-VRR-Path in Algorithm 4.

Algorithm 4: DAG-VRR-Path: DAG VRR Path Sampling

Input: Graph G , seed set S

- 1 Randomly sample root $v \in V \setminus S$ with probability proportional to $ap_v(S)$, i.e. with probability $\frac{ap_v(S)}{\sum_{u \in V \setminus S} ap_u(S)} = \frac{ap_v(S)}{\sigma^-(S)}$;
- 2 $u_0 \leftarrow v; P \leftarrow \{u_0\}; i \leftarrow 0$;
- 3 **repeat**
- 4 Sample $u_{i+1} \in N^-(u_i)$ with probability proportional to $ap_{u_{i+1}}(S) \cdot w(u_{i+1}, u_i)$, i.e. $\frac{ap_{u_{i+1}}(S) \cdot w(u_{i+1}, u_i)}{\sum_{u \in N^-(u_i)} ap_u(S) \cdot w(u, u_i)} = \frac{ap_{u_{i+1}}(S) \cdot w(u_{i+1}, u_i)}{ap_{u_i}(S)}$;
- 5 Add node u_{i+1} and edge (u_{i+1}, u_i) into path P ;
- 6 $i \leftarrow i + 1$;
- 7 **until** $u_i \in S$;
- 8 **return** a VRR path P .

Lemma 4. *If the graph G is a DAG, then any path sampled by Algorithm DAG-VRR-Path follows the subspace distribution \mathcal{P}^S .*

Therefore we can use DAG-VRR-Path sample from \mathcal{P}^S . Now we just need to analyze its running time ERPV. The generation is still similar to the LT reverse simulation. For any $u \notin S$, let $\tau(u)$ be the time needed to do a reverse simulation step from u . For the LT model, a simple binary search implementation takes $\tau(u) = O(\log_2 d_u^-)$ time, where d_u^- is the indegree of u . For an RR path P , let $\omega(P) = \sum_{u \in V(P) \setminus S} \tau(u)$ be the total time needed to generate path P . Let $\tau = \sum_{u \in V \setminus S} \tau(u)$.

Lemma 5. *Let \tilde{v} be a randomly sampled node from $V \setminus S$, with sample probability proportional to $\tau(v)$. Let P be a random VRR path generated by DAG-VRR-Path, then we have $ERPV = \mathbb{E}_{P \sim \mathcal{P}^S} [\omega(P)] = \frac{\tau}{\sigma^-(S)} \cdot \mathbb{E}_{\tilde{v}} [\rho_S(\{\tilde{v}\})]$.*

Finally, applying the above ERPV result to Theorem 1, we can obtain the following

Theorem 4. *Algorithm DAG-VRR-Path correctly samples a VRR path. The expected running time of AAIMM with DAG-VRR-Path sampling is $O\left(\frac{(q_N \log n^- + q_E \log m + \ell \log n^-) \cdot \tau \cdot \mathbb{E}_{\tilde{v}} [\rho_S(\{\tilde{v}\})]}{\text{OPT} \cdot \varepsilon^2}\right)$, where $\tau = O(\sum_{u \in V \setminus S} \log_2 d_u^-) = O(n \log n)$.*

Notice that when $q_N \geq 1$, we have $\mathbb{E}_{\tilde{v}} [\rho_S(\{\tilde{v}\})] \leq \text{OPT}$. Therefore, in this case we will have a near-linear-time algorithm, just as the original influence maximization algorithm IMM.

The above result relies that G is a DAG. When the original graph is not DAG, we can transform the graph to a DAG, similar to the DAG generation algorithm in the LDAG algorithm (Algorithm 3 in [6]). The difference is that in [6] it is generating a DAG to approximate the influence towards a root v . Instead, in our case we want to generate a DAG that approximates the influence from seed set S to other nodes. But the approach is similar, and we can efficiently implement this DAG generation process by a Dijkstra short-path-like algorithm just as in [6].

4 EXPERIMENTAL EVALUATION

4.1 Data and Algorithms

DBLP. The DBLP dataset [23] is a network of data mining, where every node is an author and every edge means the two authors collaborated on a paper. The original DBLP is a graph containing $6.546.28 \times 10^5$ nodes and $3.980.318 \times 10^6$ directed edges. However, due to the limited memory of our computer (16GB memory, 1.4GHz quad-core Intel CPU), it hardly launches the whole test on such graph. So we randomly sample $1.000.00 \times 10^5$ nodes and their $7.471.78 \times 10^5$ directed edges from the original graph, which is still the largest size of graph among all four datasets.

NetHEPT. The NetHEPT dataset [5] is extensively used in many influence maximization studies. It is an academic collaboration network from the “High Energy Physics Theory” section of arXiv from 1991 to 2003, where nodes represent the authors and each edge represents one paper co-authored by two nodes. We clean the dataset by removing duplicated edges and obtain a directed graph $G = (V, E)$, $|V| = 1.5233 \times 10^4$, $|E| = 6.2774 \times 10^4$ (directed edges).

Flixster. The Flixster dataset [1] is a network of American social movie discovery service. To transform the dataset into a weighted graph, each user is represented by a node, and a directed edge from node u to v is formed if v rates one movie shortly after u does so on the same movie. The Flixster graph contains 2.9357×10^4 nodes and $2.126.14 \times 10^5$ directed edges.

DM. The DM dataset [23] is a network of data mining researchers extracted from the ArnetMiner archive (aminer.org), where nodes present the researchers and each edge is the paper coauthorship between any two researchers. DM is the small size dataset here, which only includes 6.79×10^2 nodes and 3.374×10^3 directed edges.

4.2 Algorithms

We test all four algorithms proposed in the experiment, for the AdvIM task with different settings. Some further details of each algorithm are explained below.

AA-FF. This is the forward forest greedy algorithm. The number of forward-forest simulations of AA-FF is the same as the reverse-reachable approaches in Theorem 2. However, instead of using VRR paths, AA-FF simulate a forward forest, i.e., a set of trees, in each propagation, which is required to occupy a huge computer memory to ensure theoretical guarantee. To make it practical, we follow the standard practice in the literature and set the number of simulations as 10000 [5, 16, 28].

AA-IMM-Naive. This is the AAIMM algorithm with naive VRR path simulation, as given in Algorithm 1 and Algorithm 2. AA-IMM-Naive needs to generate plenty of RR paths for enough VRR paths since most naive RR paths can not touch the seed set S . Compared to AA-FF, AA-IMM-Naive uses much less computer memory cost to ensure the theoretical guarantee due to the RIS approach.

AA-IMM-FB. This is the AAIMM algorithm with forward-backward VRR path simulation, as given in Algorithm 1 and Algorithm 3. Unlike AA-IMM-Naive, none path won't waste in AA-IMM-FB, since all paths here are VRR paths which are randomly selected from the forward forests. To fairly compare the running time to AA-FF, We choose to sample the same number of simulations of the forward forests. The experimental results show that comparing to AA-FF, AA-IMM-FB can save more computer memory and computation power.

AA-IMM-DAG. This is the DAG-based AAIMM algorithm, as given in Algorithm 1 and Algorithm 4. Before simulation the VRR paths from DAG, we need first create a DAG as same as [6]. Compared to previous RIS approaches, AA-IMM-DAG is the fastest approach for VRR path sampling.

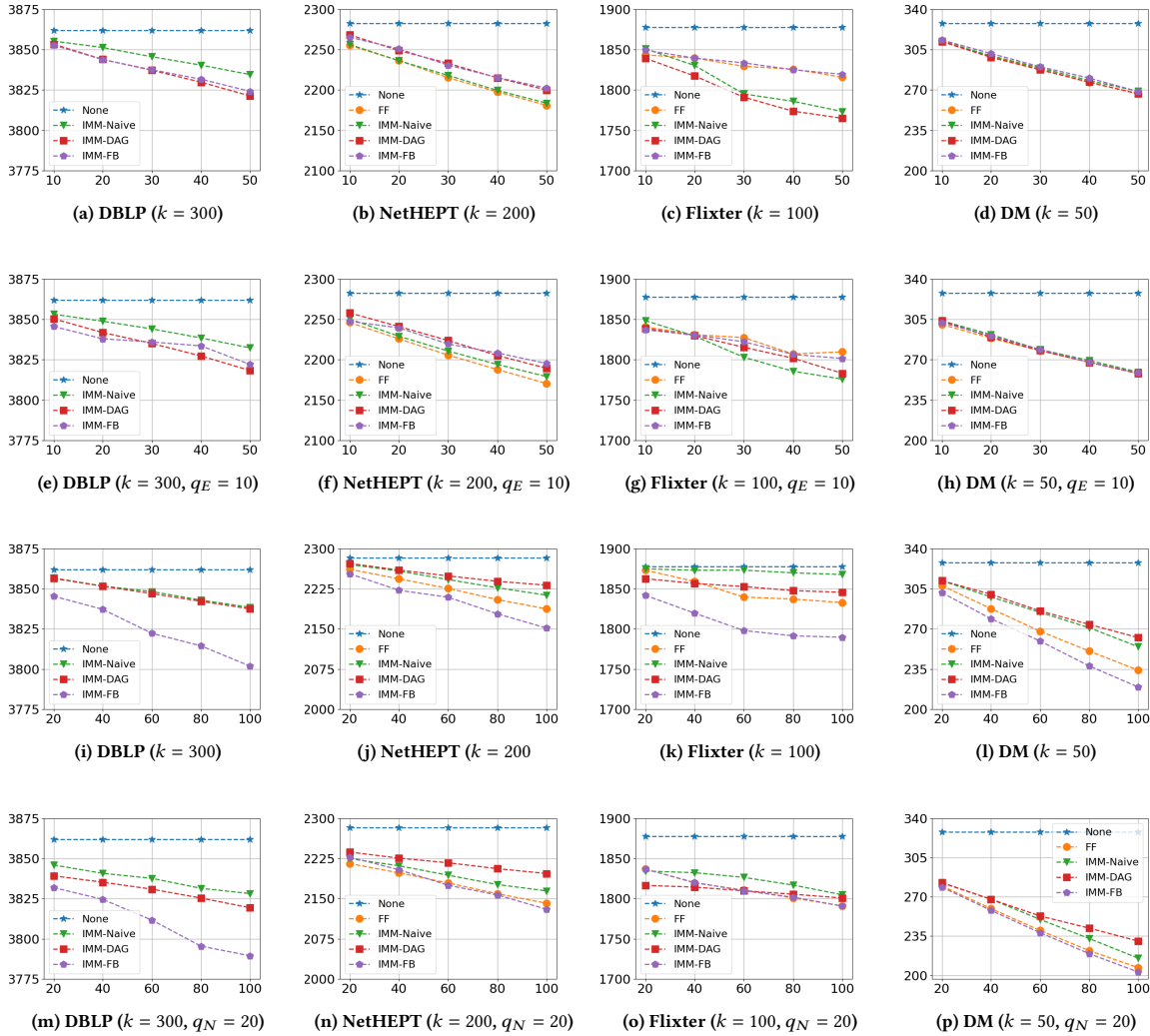


Figure 1: Evaluation budget q_N and q_E on four datasets. For (a)-(h), we fixed the q_E , and we fixed the q_N for (i)-(p). Note that the x-axis is either the edge or node budget. Once we fixed the node budget, then the x-axis is the edge budget, vice versa. The y-axis is the influence spread.

We also use 10000 Monte Carlo simulations for influence spread estimation after adversarial attacks for all above approaches.

4.3 Result

We test all four algorithms proposed in the experiment, for the Adv-IM with k seeds budget, such as AA-FF, AA-IMM-Naive, AA-IMM-FB and AA-IMM-DAG algorithms. We use $\mathcal{R} = 10000$ for the AA-FF and AA-IMM-FB on all datasets due to the high-cost computing resource and memory usage. Note that, due to the high memory cost, AA-FF can not finish the whole test even $\mathcal{R} = 10000$.

In all tests, we set the seed set $k = 50, 100, 200, 300$ for DM, Flixster, NetHEPT and DBLP respectively, and we also test different combinations of q_N and q_E .

Influence Spread Performance. From Figure 1, it is not hard to see that the influence of the selected seed set is decreasing while increasing either the node budget q_N or the edge budget q_E over all 16 tasks. On DBLP, we can see that AA-IMM-FB > AA-IMM-DAG > AA-IMM-DAG based on the performance on influence reduction, and AA-FF can not finish the test with $\mathcal{R} = 10000$. NetHEPT have the similar ranking results as DBLP that we have AA-IMM-FB = AA-FF > AA-IMM-Naive > AA-IMM-DAG in most cases. However, on Flixster, the ranking becomes very different. AA-IMM-DAG becomes the best in most cases, and AA-FF and AA-IMM-FB show the worst influence reduction performance in Figures 1 (c) and (g). On DM, all methods perform close to each other. In summary, the results demonstrate that all algorithms perform close to each other. In general, either AA-IMM-DAG and AA-FF can achieve the best performance in different tasks. In this case, the running time becomes the key while applying the algorithms in real applications.

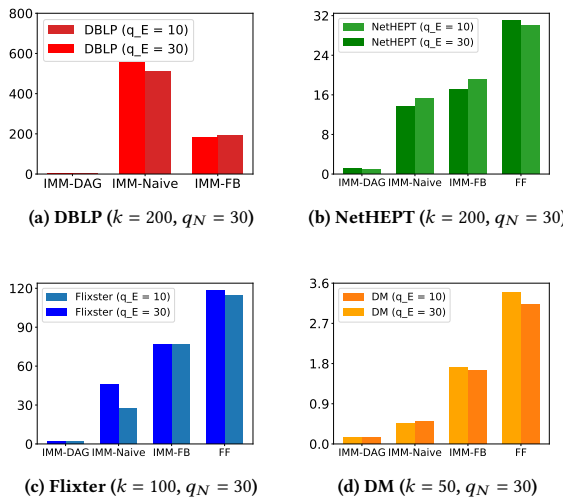


Figure 2: Running time analysis. For all datasets, the node budget is fixed as 30. The y-axis is the running time (seconds).

Running time. Figure 2 reports the running time of all the tested algorithms on the four datasets. One clear conclusion is that all IMM algorithms are much more efficient than AA-FF that even fails to

finish the test on DBLP. Among three RIS algorithms, it is obvious that AA-IMM-DAG is the fastest algorithm, AA-IMM-Naive is the second, and the AA-IMM-FB is the slowest one. However, from DBLP’s results, AA-IMM-Naive is slower than AA-IMM-FB, which is not due to the limited number of simulations of the AA-IMM-FB, i.e., $\mathcal{R} = 10000$. More importantly, AA-IMM-DAG is at least 10 times faster than all other algorithms, including other RIS-based approaches. After combining the influence spread and running time performance together, we recommend AA-IMM-DAG and AA-IMM-FB algorithms to be the best two choices for AdvIM, and AA-FF to be the worst choice due to the cost of high computer memory and high running time.

4.4 Discussion

From the experiments, we found several interesting aspects. The most important is why AA-FF algorithm took so much memory and computing resource compared to VRR path simulation approaches. The primary reason is that AA-FF algorithm takes too much memory spaces. For RR path simulation, no matter how big the original seed set is, we only save one single path per simulation. However, in each AA-FF simulation, the size of the forest is related not only to the graph’s properties but also to the size of the target seed set. While the target seed set contains 100 nodes, there are 100 sub-tree in each simulation by the AA-FF algorithm. It means AA-FF can not be practical in a real application. For example, if we want to stop COVID-19 with a virus spread graph, the seed sets maybe thousands in a vast network. In this case, VRR-based path simulation is the best for a large graph simulation for Adv-IM.

5 CONCLUSION

In this paper, we study the adversarial attack on influence maximization (AdvIM) task, and propose efficient algorithms for solving AdvIM problems. We adapt the RIS approach to improve the efficiency for the AdvIM task. The experimental results demonstrate that our algorithms are more effective and efficient than previous approaches. There are several future directions from this research. One direction is to attack the influence maximization on uncertainty networks or dynamic networks. We can also study the blocking the influence propagation without knowing the seed set. Another direction is to sample less number of forward forests with theoretical analysis. Adversarial attack on other influence propagation models may also be explored.

REFERENCES

- [1] Nicola Barbieri, Francesco Bonchi, and Giuseppe Manco. 2012. Topic-aware social influence propagation models. In *ICDM’12*. IEEE.
- [2] Smriti Bhagat, Amit Goyal, and Laks V. S. Lakshmanan. 2012. Maximizing product adoption in social networks. In *WSDM*. ACM.
- [3] Christian Borgs, Michael Brautbar, Jennifer Chayes, and Brendan Lucier. 2014. Maximizing social influence in nearly optimal time. In *ACM-SIAM (SODA ’14)*.
- [4] Ceren Budak, Divyakant Agrawal, and Amr El Abbadi. 2011. Limiting the spread of misinformation in social networks. In *WWW11*.
- [5] Ning Chen. 2008. On the approximability of influence in social networks. In *SODA ’08*. Society for Industrial and Applied Mathematics.
- [6] Wei Chen, Alex Collins, Rachel Cummings, Te Ke, Zhenming Liu, David Rincon, Xiaorui Sun, Yajun Wang, Wei Wei, and Yifei Yuan. 2011. Influence maximization in social networks when negative opinions may emerge and propagate. In *SDM*.
- [7] Wei Chen, Tian Lin, Zihan Tan, Mingfei Zhao, and Xuren Zhou. 2016. Robust Influence Maximization. In *KDD*.
- [8] Wei Chen, Yajun Wang, and Siyu Yang. 2009. Efficient influence maximization in social networks. In *KDD*.

- [9] Wei Chen, Yifei Yuan, and Li Zhang. 2010. Scalable Influence Maximization in Social Networks under the Linear Threshold Model. In *ICDM*.
- [10] Pedro Domingos and Matthew Richardson. 2001. Mining the network value of customers. In *KDD*.
- [11] Marshall L Fisher, George L Nemhauser, and Laurence A Wolsey. 1978. An analysis of approximations for maximizing submodular set functions II. In *Polyhedral combinatorics*. Springer.
- [12] Lifang He, Chun-Ta Lu, Jiaqi Ma, Jianping Cao, Linlin Shen, and Philip S Yu. 2016. Joint community and structural hole spanner detection via harmonic modularity. In *SIGKDD ACM*.
- [13] X. He and D. Kempe. 2016. Robust Influence Maximization. In *KDD*.
- [14] Xinran He, Guojie Song, Wei Chen, and Qingye Jiang. 2012. Influence Blocking Maximization in Social Networks under the Competitive Linear Threshold Model. In *SDM12*.
- [15] Kyomin Jung, Wooram Heo, and Wei Chen. 2012. IRIE: Scalable and Robust Influence Maximization in Social Networks. In *ICDM*.
- [16] David Kempe, Jon M. Kleinberg, and Éva Tardos. 2003. Maximizing the spread of influence through a social network. In *KDD*.
- [17] Elias Boutros Khalil, Bistra Dilkina, and Le Song. 2014. Scalable diffusion-aware optimization of network topology. In *Proceedings of the 20th ACM SIGKDD international conference on Knowledge discovery and data mining*. 1226–1235.
- [18] Jure Leskovec, Andreas Krause, Carlos Guestrin, Christos Faloutsos, Jeanne M. VanBriesen, and Natalie S. Glance. 2007. Cost-effective outbreak detection in networks. In *KDD*.
- [19] Wei Lu, Wei Chen, and Laks VS Lakshmanan. 2015. From competition to complementarity: comparative influence diffusion and maximization. *PVLDB* (2015).
- [20] G. L. Nemhauser, L. A. Wolsey, and M. L. Fisher. 1978. *An analysis of the approximations for maximizing submodular set functions*. Mathematical Programming.
- [21] Hung T. Nguyen, My T. Thai, and Thang N. Dinh. 2016. Stop-and-Stare: Optimal Sampling Algorithms for Viral Marketing in Billion-Scale Networks. In *Proc. ACM SIGMOD*. 695–710.
- [22] Matthew Richardson and Pedro Domingos. 2002. Mining knowledge-sharing sites for viral marketing. In *KDD*.
- [23] Jie Tang, Jimeng Sun, Chi Wang, and Zi Yang. 2009. Social influence analysis in large-scale networks. In *Proceedings of the 15th ACM SIGKDD international conference on Knowledge discovery and data mining*. 807–816.
- [24] Jing Tang, Xueyan Tang, Xiaokui Xiao, and Junsong Yuan. 2018. Online Processing Algorithms for Influence Maximization. In *Proc. ACM SIGMOD*. 991–1005.
- [25] Youze Tang, Yanchen Shi, and Xiaokui Xiao. 2015. Influence maximization in near-linear time: a martingale approach. In *SIGMOD*.
- [26] Youze Tang, Xiaokui Xiao, and Yanchen Shi. 2014. Influence maximization: near-optimal time complexity meets practical efficiency. In *SIGMOD*.
- [27] Chayant Tantipathananandh, Tanya Berger-Wolf, and David Kempe. 2007. A framework for community identification in dynamic social networks. In *KDD'07*.
- [28] Chi Wang, Wei Chen, and Yajun Wang. 2012. Scalable influence maximization for independent cascade model in large-scale social networks. *DMKD* (2012).

APPENDIX

A FORWARD FOREST ALGORITHM

In this section, we provide a greedy approach with theoretical guarantees by estimating the forward forest simulation, as given in Algorithm 5. Unlike the naive greedy approaches with Monte Carlo simulations, we further provide the new theoretical analysis based on IMM for AA-FF, which can give a more precise and less number of simulations. Algorithm 5 has two phases too. In Phase 1, we generate θ forward forests \mathcal{F} , where θ is computed to guarantee the approximation with high probability. In Phase 2, we use the greedy algorithm to find the q_N nodes and q_E edges that cover the most number of forest forests. Phase 1 here also follows the IMM structure to estimate a lower bound of the optimal value, which is used to determine the number of the forward forests needed for the theoretical guarantee. Unlike all RIS approaches, AA-FF samples a forest started from the seed set S per time. In order to save the forward forests, it requires a huge memory compared to the RIS approaches. So, in practice, we simulate a small number that is far away from the required number to ensure the theoretical guarantee, as shown below.

Theorem 5. *Let A^* be the optimal solution of the AdvIM. For every $\varepsilon > 0$ and $\ell > 0$, with probability at least $1 - \frac{1}{n^\ell}$, the output A^0 of the Forward Forest Simulation Adversarial Attacks algorithm AA-FF satisfies*

$$\rho_S(A^0) \geq \left(\frac{1}{2} - \varepsilon\right) \rho_S(A^*),$$

In this case, the total running time for AA-FF is

$$O\left(\frac{(q_N \log n^- + q_E \log m + \ell \log n^-) \cdot n}{\text{OPT} \cdot \varepsilon^2} \cdot (\text{EFF}(S) + q \cdot \text{EFD}(S))\right). \quad (5)$$

PROOF. First, based on the definition of the $\hat{\rho}(S, \mathcal{L})$, we can define the influence deduction function $\rho_S(A)$. Because of $|\Gamma(L_i, S) - \Gamma(L_i \setminus A, S)|$ is monotone as a function of A , so $\rho_S(A)$ is also monotone. In this case, we can apply Lemma 6 to ensure the correctness of the AA-FF algorithm. To ensure the first two conditions of Lemma 6, we need to generate enough live-edge graphs, and the number of the graphs is referred by Lemma 7. However, Lemma 7 is two-sided concentration inequality based on Fact 1. In fact, Lemma 6 only need one-sided concentration inequality based on Fact 2. So, we can use Lemma 8 and Fact 2, and we have $\delta_1 = \delta_2 = \frac{1}{2n^\ell}$. Now, we have a conclusion: let $\alpha = \sqrt{\ell \ln n^- + \ln 2}$, $\beta = \sqrt{1/2 \cdot (\ln((\binom{n^-}{q_N}) \binom{m}{q_E})) + \ell \ln n^- + \ln 2}$, then while $\theta \geq 3n(1/2 \cdot \alpha + \beta)^2 / (\text{OPT} \cdot \varepsilon^2)$, two conditions of Lemma 6 satisfies, and we have FS-Adv-Greedy returns $A^0(\mathcal{L})$ with at least $1 - \frac{1}{n^\ell}$ probability satisfying $\rho_S(A^0) \geq (\frac{1}{2} - \varepsilon) \rho_S^*(A^*)$.

Next, we prove the time complexity of the AA-FF. Similar to the above argument, we need

$$O\left(\frac{(q_N \log n^- + q_E \log m + \ell \log n^-) \cdot \sigma^-(S)}{\text{OPT} \cdot \varepsilon^2}\right).$$

number of forward forests, where OPT is the optimal solution of the influence reduction problem.

Let $\text{EFF}(S)$ be the mean time of generating a forward forest from seed set S , and $\text{EFD}(S)$ be the mean depth of a forward forest from S

Algorithm 5: AA-FF: Adversarial Attack Forward-Forest Greedy Algorithm

Input: Graph $G = (V, E)$, LT influence weights $\{w(u, v)\}_{(u, v) \in E}$, budget q_N for nodes and q_E for edges, seed set S

Output: attack set A

- 1 Initialization: attack set $A \leftarrow \emptyset$, forest set $\mathcal{F} \leftarrow \emptyset$, influence score array $I(a) \leftarrow 0$, for all $a \in V \cup E$;
- 2 **for** $i=1$ to θ **do**
- 3 Forward propagate a new forest F_i from seed set S by using LT model in G ;
 $\mathcal{F} \leftarrow \mathcal{F} \cup F_i$;
- 4 Calculate the influence score $I_i(a)$ of each node or edge z in F_i , Using DFS on F_i ;
- 5 Update I : for all a in F_i , $I(a) \leftarrow I(a) + I_i(a)$;
- 6 **while** $q_N + q_E > 0$ **do**
- 7 **if** $q_E == 0$ **then**
 $a \leftarrow \text{argmax}_{a \in V} I(a)$;
- 8 **else if** $q_N == 0$ **then**
 $a \leftarrow \text{argmax}_{a \in E} I(a)$;
- 9 **else**
 $a \leftarrow \text{argmax}_{a \in V \cup E} I(a)$;
- 10 **if** $a \in V$ **then**
 $q_N \leftarrow q_N - 1$;
- 11 **else**
 $q_E \leftarrow q_E - 1$;
- 12 **for** each forest $F_i \in \mathcal{F}$ containing a **do**
 $I(z) \leftarrow I(z) - I_i(z)$;
 $I(z) \leftarrow I(z) - I_i(a)$;
 $A \leftarrow A \cup a$;
- 13 **return** A .

(depth of a forest is the length of the longest path in a forest, and the expectation is taking over the randomness of the forest). According the discussion above, average generation of one forest takes $\text{EFF}(S)$ time, and update on a forest would take $O(\text{EFF}(S) + q \cdot \text{EFD}(S))$ time, so the total running time is

$$O\left(\frac{(q_N \log n^- + q_E \log m + \ell) \cdot \sigma^-(S)}{\text{OPT} \cdot \varepsilon^2} \cdot (\text{EFF}(S) + q \cdot \text{EFD}(S))\right).$$

Note that $\text{EFF}(S) + q \cdot \text{EFD}(S)$ is dynamic, which depends on the seed set S and the properties of graph G . \square

B PROOF - SUPPLEMENTARY

Fact 1. (Chernoff bound) Let X_1, X_2, \dots, X_R be R independent random variables and with X_i having range $[0, 1]$. Let $X = \sum_{i=1}^R X_i / R$,

for any $0 < \gamma < 1$, we have

$$\Pr\{|X - \mathbb{E}[X]| \geq \gamma \cdot \mathbb{E}[X]\} \leq 2 \exp\left(-\frac{\gamma^2 \mathbb{E}[X]}{3}\right).$$

Fact 2. (Chernoff bound) Let X_1, X_2, \dots, X_R be R independent random variables and with X_i having range $[0, 1]$. and there exists $\mu \in [0, 1]$ making $\mathbb{E}[X_i] = \mu$ for any $i \in [R]$. Let $Y = \sum_{i=1}^R X_i$, for any $\gamma > 0$,

$$\Pr\{Y - t\mu \geq \gamma \cdot t\mu\} \leq \exp\left(-\frac{\gamma^2}{2 + \frac{2}{3}\gamma} t\mu\right).$$

For any $0 < \gamma < 1$,

$$\Pr\{Y - t\mu \leq -\gamma \cdot t\mu\} \leq \exp\left(-\frac{\gamma^2}{2} t\mu\right).$$

Lemma 1. Influence reduction $\rho_S(A)$ for the LT model satisfies monotonicity and submodularity.

PROOF. The proof is based on the live-edge graph representation of the LT model. The proof for the monotonicity property is straightforward, so we focus on the submodularity property. Let A_1 and A_2 be two attack sets with $A_1 \subseteq A_2$, and $x \in ((V \setminus S) \cup E) \setminus A_2$. According to the definition of the influence reduction, we have

$$\begin{aligned} \rho_S(A_1 \cup \{x\}) - \rho_S(A_1) &\geq \rho_S(A_2 \cup \{x\}) - \rho_S(A_2) \\ \Leftrightarrow \mathbb{E}_L[|\Gamma(L, S) \setminus \Gamma(L \setminus A_1 \setminus \{x\}, S)|] - \mathbb{E}_L[|\Gamma(L, S) \setminus \Gamma(L \setminus A_1, S)|] \\ &\geq \mathbb{E}_L[|\Gamma(L, S) \setminus \Gamma(L \setminus A_2 \setminus \{x\}, S)|] - \mathbb{E}_L[|\Gamma(L, S) \setminus \Gamma(L \setminus A_2, S)|]. \end{aligned}$$

Then it is sufficient to show that for any fixed live-edge graph L , for every node $v \in V \setminus S$, if $v \in \Gamma(L, S) \setminus \Gamma(L \setminus A_2 \setminus \{x\}, S)$ but $v \notin \Gamma(L, S) \setminus \Gamma(L \setminus A_1, S)$, then $v \in \Gamma(L, S) \setminus \Gamma(L \setminus A_1 \setminus \{x\}, S)$ but $v \notin \Gamma(L, S) \setminus \Gamma(L \setminus A_1, S)$. Now suppose that $v \in \Gamma(L, S) \setminus \Gamma(L \setminus A_2 \setminus \{x\}, S)$ but $v \notin \Gamma(L, S) \setminus \Gamma(L \setminus A_1, S)$. This means that v cannot be reached from S in L after $A_2 \cup \{x\}$ are removed from L , but v can be reached from S if we only remove A_2 from L . Since $A_1 \subseteq A_2$, we have that when we remove A_1 from L , v can still be reached from S , i.e. $v \notin \Gamma(L, S) \setminus \Gamma(L \setminus A_1, S)$. Since after further removing x , v cannot be reached from S after we already remove A_2 , there is at least one path P from S to v that passes through x but not through any element in A_2 . By the live-edge graph construction in the LT model, actually there is at most one path from S to v . Therefore, P is the unique path from S to v , and none of the nodes or edges in A_2 are on P but x is on P . Since $A_1 \subseteq A_2$, we know that after removing A_1 , P still exists but after removing x , P no longer exists and there is no path from S to v any more. This means that $v \in \Gamma(L, S) \setminus \Gamma(L \setminus A_1 \setminus \{x\}, S)$ but $v \notin \Gamma(L, S) \setminus \Gamma(L \setminus A_1, S)$. This is what we want, and the lemma holds. \square

Lemma 2. For any given seed set S and attack set A ,

$$\begin{aligned} \rho_S(A) &= n^- \cdot \mathbb{E}_L[\mathbb{I}\{A \cap VE(P_L^S) \neq \emptyset\}] \\ &= \sigma^-(S) \cdot \mathbb{E}_L[\mathbb{I}\{A \cap VE(P_L) \neq \emptyset\} \mid S \cap VE(P_L) \neq \emptyset]. \end{aligned}$$

PROOF. By definition, we have

$$\begin{aligned}
\rho_S(A) &= \mathbb{E}_L[|\{v \in V \setminus S \mid v \in \Gamma(L, S) \wedge v \notin \Gamma(L \setminus A, S)\}|] \\
&= \mathbb{E}_L\left[\sum_{v \in V \setminus S} \mathbb{I}\{v \in \Gamma(L, S) \wedge v \notin \Gamma(L \setminus A, S)\}\right] \\
&= \mathbb{E}_L[n^- \cdot \mathbb{E}_{v \sim \mathcal{U}(V \setminus S)}[\mathbb{I}\{v \in \Gamma(L, S) \wedge v \notin \Gamma(L \setminus A, S)\}]] \\
&= n^- \cdot \mathbb{E}_{L, v \sim \mathcal{U}(V \setminus S)}[\mathbb{I}\{A \cap P_L^S(v) \neq \emptyset\}] \\
&= n^- \cdot \Pr_{L, v \sim \mathcal{U}(V \setminus S)}\{S \cap P_L(v) \neq \emptyset\} \\
&\quad \cdot \mathbb{E}_{L, v \sim \mathcal{U}(V \setminus S)}[\mathbb{I}\{A \cap P_L(v) \neq \emptyset\} \mid S \cap P_L(v) \neq \emptyset] \\
&= \sigma^-(S) \cdot \mathbb{E}_{L, v \sim \mathcal{U}(V \setminus S)}[\mathbb{I}\{A \cap P_L(v) \neq \emptyset\} \mid S \cap P_L(v) \neq \emptyset] \quad (6) \\
&= \sigma^-(S) \cdot \mathbb{E}_{P \sim \mathcal{P}^S}[\mathbb{I}\{A \cap P \neq \emptyset\}], \quad (7)
\end{aligned}$$

where $\mathcal{U}(V \setminus S)$ denote the uniform distribution among all nodes in $V \setminus S$. Eq. (6) is due to the original RR set connection with the influence spread [3, 25, 26], which shows that $\Pr_{L, v \sim \mathcal{U}(V \setminus S)}\{S \cap P_L(v) \neq \emptyset\} = \sigma^-(S)/n^-$. Eq. (7) follows from the subspace definition of \mathcal{P}^S . \square

Lemma 3. For every $\varepsilon > 0$ and $\ell > 0$, to guarantee the approximation ratio with probability at least $1 - \frac{1}{n^\ell}$, the number of VRR paths needed by AAIMM is $O\left(\frac{(q_N \log n^- + q_E \log m + \ell \log n^-) \cdot \sigma^-(S)}{\text{OPT} \cdot \varepsilon^2}\right)$.

PROOF. When working on the subspace \mathcal{P}^S in AAIMM, we are working on the objective function $n^- \cdot \mathbb{E}_{P \sim \mathcal{P}^S}[\mathbb{I}\{A \cap VE(P) \neq \emptyset\}]$ (e.g. see lines 3, 8, and 9). Thus by Lemma 2, the real objective function $\rho_S(A)$ is only a fraction $\frac{\sigma^-(S)}{n^-}$ of the new objective function. Let OPT' be the optimal value of the new objective function. Applying the analysis of IMM [25], we know that the number of VRR path samples that we need in the subspace \mathcal{P}^S is

$$O\left(\frac{(q_N \log n^- + q_E \log m + \ell \log n^-) \cdot n^-}{\text{OPT}' \cdot \varepsilon^2}\right). \quad (8)$$

Because $\text{OPT} = \frac{\sigma^-(S)}{n^-} \cdot \text{OPT}'$, the above formula is changed to

$$O\left(\frac{(q_N \log n^- + q_E \log m + \ell \log n^-) \cdot \sigma^-(S)}{\text{OPT} \cdot \varepsilon^2}\right), \quad (9)$$

\square

Theorem 1. For every $\varepsilon > 0$ and $\ell > 0$, with probability at least $1 - \frac{1}{n^\ell}$, the output A^o of the AAIMM algorithm framework satisfies $\rho_S(A^o) \geq \left(\frac{1}{2} - \varepsilon\right) \rho_S(A^*)$. In this case, the expected running time for AAIMM is $O\left(\frac{(q_N \log n^- + q_E \log m + \ell \log n^-) \cdot \sigma^-(S)}{\text{OPT} \cdot \varepsilon^2} \cdot \text{ERPV}\right)$, where ERPV is the mean time of generating a VRR path.

PROOF. Following [11], our NodeEdgeSelection procedure finds an attack set that covers at least $1/2$ of all the VRR paths generated. Then following the standard analysis of IMM, our AAIMM algorithm provides $1/2 - \varepsilon$ approximation with probability at least $1 - \frac{1}{n^\ell}$. The expected running time follows Lemma 3 and the definition of ERPV . \square

Theorem 2. Naive VRR path sampling (Algorithm 2) correctly samples a VRR path. The expected running time of AAIMM with naive VRR path sampling (Algorithm 2) is

$$O\left(\frac{(q_N \log n^- + q_E \log m + \ell \log n^-) \cdot n^-}{\text{OPT} \cdot \varepsilon^2} \cdot \text{ERP}\right). \quad (3)$$

PROOF. It is obvious that the naive VRR path sampling will return a VRR path according to distribution \mathcal{P}^S . We just need to prove that $\text{ERP} = \text{ERP} \cdot n^- / \sigma^-(S)$, and the rest follows from Theorem 1. For each live-edge graph L , if we randomly select a root $v \in V \setminus S$, then with probability $(|\Gamma(L, S)| - |S|)/n^-$, v is reachable from S in L , which means the RR path from v will intersect with S on this live-edge graph L . Taking expectation over L , we know that the probability of an RR path is valid is $\mathbb{E}_L[(|\Gamma(L, S)| - |S|)/n^-] = \sigma^-(S)/n^-$. Therefore, on average we need to generate $n^- / \sigma^-(S)$ RR paths to get one VRR path, which means $\text{ERP} = \text{ERP} \cdot n^- / \sigma^-(S)$. \square

Theorem 3. Forward-backward VRR path sampling (Algorithm 3) correctly samples a VRR path. The expected running time of AAIMM with forward-backward VRR path sampling (Algorithm 3) is

$$O\left(\frac{(q_N \log n^- + q_E \log m + \ell \log n^-) \cdot \sigma^-(S)}{\text{OPT} \cdot \varepsilon^2} \cdot \text{EFF}(S)\right). \quad (4)$$

PROOF. For any fixed live-edge graph L , conditioned on sampling a VRR path, random sampling a root v is equivalent of sampling from $\Gamma(L, S) \setminus S$ uniformly at random, which is exactly from the forward forest generated by forward simulation from S . Thus, the forward-backward sampling method is correct. \square

Lemma 4. If the graph G is a DAG, then any path sampled by Algorithm DAG-VRR-Path follows the subspace distribution \mathcal{P}^S .

PROOF. First, notice that Algorithm DAG-VRR-Path re-weights the incoming edges (u, v) of every node v according to the activation probability $\text{ap}_u(S)$. Therefore any node u that cannot be activated by S will cause (u, v) to have zero weight, and thus will not be sampled in the reverse sampling process. Therefore, the reverse sampling process will always samples toward the seed set, and since the graph has no cycle, it will always end at a seed node in S . This means that the output of DAG-VRR-Path is always a VRR path. We just need to show that it follows the subspace distribution \mathcal{P}^S .

To show that its distribution is the same as \mathcal{P}^S , all we need to show is that if we have two paths P_1 and P_2 that both starts from a seed node in S , then the ratio of the probabilities of generating these two paths by the above procedure is the same as the ratio in the original RR path space. Let $P_1 = (u_s, u_{s-1}, \dots, u_0)$ and $P_2 = (z_t, z_{t-1}, \dots, z_0)$, with $u_0, z_0 \in V \setminus S$ and $u_s, z_t \in S$. Let $\pi(P)$ be the probability of sampling the RR path P in the original space. Then we have $\pi(P_1) = \frac{1}{n^-} \prod_{i=1}^s w(u_i, u_{i-1})$, and $\pi(P_2) = \frac{1}{n^-} \prod_{j=1}^t w(z_j, z_{j-1})$. So the ratio is

$$\frac{\pi(P_1)}{\pi(P_2)} = \frac{\prod_{i=1}^s w(u_i, u_{i-1})}{\prod_{j=1}^t w(z_j, z_{j-1})}. \quad (10)$$

Now let $\pi'(P)$ be the probability of generating path P by **DAG-VRR-Path**. Then we have

$$\pi'(P_1) = \frac{\text{ap}_{u_0}(S)}{\sigma^-(S)} \prod_{i=1}^s \frac{\text{ap}_{u_i}(S) \cdot w(u_i, u_{i-1})}{\text{ap}_{u_{i-1}}(S)} = \frac{\prod_{i=1}^s w(u_i, u_{i-1})}{\sigma^-(S)}, \quad (11)$$

Where the above derivation also uses the fact that $u_s \in S$ and thus $\text{ap}_{u_s}(S) = 1$. Similarly, we have

$$\pi'(P_2) = \frac{\text{ap}_{z_0}(S)}{\sigma^-(S)} \prod_{j=1}^t \frac{\text{ap}_{z_j}(S) \cdot w(z_j, z_{j-1})}{\text{ap}_{z_{j-1}}(S)} = \frac{\prod_{j=1}^t w(z_j, z_{j-1})}{\sigma^-(S)}. \quad (12)$$

Therefore, clearly $\pi'(P_1)/\pi'(P_2) = \pi(P_1)/\pi(P_2)$, and the above procedure correctly generates a VRR path from the subspace \mathcal{P}^S . \square

Lemma 5. Let \tilde{v} be a randomly sampled node from $V \setminus S$, with sample probability proportional to $\tau(v)$. Let P be a random VRR path generated by **DAG-VRR-Path**, then we have $\text{ERPV} = \mathbb{E}_{P \sim \mathcal{P}^S} [\omega(P)] = \frac{\tau}{\sigma^-(S)} \cdot \mathbb{E}_{\tilde{v}} [\rho_S(\{\tilde{v}\})]$.

PROOF. For a fixed RR path P , let $p(P)$ be the probability $\tilde{v} \in V(P)$. Then it is clear that

$$p(P) = \mathbb{E}_{\tilde{v}} [\mathbb{I}\{\tilde{v} \in V(P)\}] = \frac{\omega(P)}{\tau}.$$

Now let P be a random VRR path generated by **DAG-VRR-Path**. Then

$$\begin{aligned} \mathbb{E}_{P \sim \mathcal{P}^S} [\omega(P)] &= \tau \cdot \mathbb{E}_{P \sim \mathcal{P}^S} [p(P)] = \tau \cdot \mathbb{E}_{P \sim \mathcal{P}^S} [\mathbb{E}_{\tilde{v}} [\mathbb{I}\{\tilde{v} \in V(P)\}]] \\ &= \tau \cdot \mathbb{E}_{\tilde{v}} [\mathbb{E}_{P \sim \mathcal{P}^S} [\mathbb{I}\{\tilde{v} \in V(P)\}]] = \frac{\tau}{\sigma^-(S)} \cdot \mathbb{E}_{\tilde{v}} [\rho_S(\{\tilde{v}\})], \end{aligned}$$

where the last equality is by Lemma 2. \square

Lemma 6. For any $\varepsilon > 0$, $\varepsilon_1 \in (0, \varepsilon/(1-1/2))$, for any $\delta_1, \delta_2 > 0$, if (a) $\Pr_{\omega \in \Omega} \{\rho_S(A^*, \omega) \geq (1-\varepsilon_1) \cdot OPT\} \geq 1-\delta_1$; (b) for every bad A to ε , (a) $\Pr_{\omega \in \Omega} \{\rho_S(A\omega) \geq (1-1/2)(1-\varepsilon_1) \cdot OPT\} \leq \delta_2 / \binom{n}{q_N} \binom{m}{q_E}$; (c) for all $\omega \in \Omega$, $\rho_S(A, \omega)$ is submodular to S , then, with at least $1 - \delta_1 - \delta_2$, the greedy output $A^0(\omega)$ of $\rho_S(\cdot, \omega)$ holds

$$\Pr_{\omega \in \Omega} \{\rho_S(A^0, \omega) \geq (1/2 - \varepsilon) \cdot OPT\} \leq 1 - \delta_1 - \delta_2,$$

PROOF. Because $\rho_S(A^0, \omega)$ is both monotone and submodular, then we have:

$$\rho_S(A^0, \omega) \geq \frac{1}{2} \rho_S(A^*, \omega).$$

Based on the condition (a) in this lemma, we know it holds at least $1 - \delta_1$ probability,

$$\rho_S(A^0, \omega) \geq \frac{1}{2} \rho_S(A^*, \omega) \geq \frac{1}{2} (1 - \varepsilon_1) \cdot OPT.$$

Based on the condition (b) in this lemma, existing a bad A causing $\rho_S(A, \omega) \geq \frac{1}{2} (1 - \varepsilon_1) \cdot OPT$ with at most δ_2 probability. Because of at most $\binom{n}{q_N} \binom{m}{q_E}$ sets with q_N nodes and q_E edges, for every bad S , the probability would not be more than $\delta_2 / \binom{n}{q_N} \binom{m}{q_E}$. Then, based on the union bound, we know that, with at least $1 - \delta_1 - \delta_2$ probability, $\rho_S(A^0)$ is not bad, which means $\rho_S(A^0, \omega) \geq (1/2 - \varepsilon) \cdot OPT$. \square

Lemma 7. For any attack set A , the original greedy algorithm returns $\hat{\rho}_S(A)$ non-bias influence estimation $\rho_S(A)$. For any $0 < \delta < 1$ and $0 < \gamma < 1$, while $R \geq \frac{3n^-}{\gamma^2 \rho_S(A)} \ln(\frac{2}{\delta})$, we have $\Pr\{|\hat{\rho}_S(A) - \rho_S(A)| \leq \gamma \cdot \rho_S(A)\} \geq 1 - \delta$. If $f_v(A)$ spends constant time, the time complexity is $O(n^- R)$.

PROOF. Let X_i become the percentage of total removed nodes among all nodes in i -th simulation. Then, we have (a) $X_i \in [0, 1]$; (b) $\mathbb{E}[X_i] = \rho_S(A)/n^-$; and (c) $\hat{\rho}_S(A) = \sum_{i=1}^R n^- X_i / R$. Let $X = \sum_{i=1}^R X_i = \hat{\rho}_S(A) \cdot R / n^-$. First,

$$\mathbb{E}[\hat{\rho}_S(A)] = \mathbb{E}\left[\frac{\sum_{i=1}^R n^- X_i}{R}\right] = \frac{\sum_{i=1}^R n^- \mathbb{E}[X_i]}{R} = \rho_S(A).$$

Then, $\hat{\rho}_S(A)$ is non-bias estimation $\rho_S(A)$. Next, due to simulations are independent between each other, based on the Chernoff bound (Fact 1), we have

$$\begin{aligned} &\Pr\{|\hat{\rho}_S(A) - \rho_S(A)| \leq \gamma \cdot \rho_S(A)\} \\ &= \Pr\{|R \cdot \hat{\rho}_S(A)/n^- - R \cdot \rho_S(A)/n^-| \leq \gamma \cdot R \cdot \rho_S(A)/n^-\} \\ &= \Pr\{|X - \mathbb{E}[X]| \leq \gamma \cdot \mathbb{E}[X]\} \\ &= 1 - \Pr\{|X - \mathbb{E}[X]| > \gamma \cdot \mathbb{E}[X]\} \\ &\geq 1 - 2 \exp\left(-\frac{\gamma^2 \mathbb{E}[X]}{3}\right) = 1 - 2 \exp\left(-\frac{\gamma^2 R \cdot \rho_S(A)}{3}\right) \end{aligned}$$

The last step is based on Chernoff bound. Finally, let $R \geq \frac{3n^-}{\gamma^2 \rho_S(A)} \ln(\frac{2}{\delta})$, we have $\Pr\{|\hat{\rho}_S(A) - \rho_S(A)| \leq \gamma \cdot \rho_S(A)\} \geq 1 - \delta$. \square

Lemma 8. [25]. For any $\varepsilon > 0$, $\varepsilon_1 \in (0, \varepsilon/(1-1/2))$, for any $\delta_1, \delta_2 > 0$, let

$$\theta_1 = \frac{2n^- \cdot \ln(1/\delta_1)}{OPT \cdot \varepsilon_1^2}, \quad \theta_2 = \frac{n^- \cdot \ln(\binom{n}{q_N} \binom{m}{q_E}) / \delta_2}{OPT \cdot (\varepsilon - 1/2 \cdot \varepsilon_1)^2}.$$

For any fixed $\theta \geq \theta_1$, we have

$$\Pr_{\omega \in \Omega} \{\rho_S(A^*, \omega) \geq (1 - \varepsilon_1) \cdot OPT\} \geq 1 - \delta_1.$$

For any fixed $\theta \geq \theta_2$ and for every bad A to ε , we have

$$\Pr_{\omega \in \Omega} \{\rho_S(A, \omega) \geq (1 - 1/2)(1 - \varepsilon_1) \cdot OPT\} \leq \frac{\delta_2}{\binom{n}{q_N} \binom{m}{q_E}}.$$